Multiscale modeling of precipitation in Fe-Cu-Ni-Mn alloys: bridging kinetic Monte Carlo and phase-field simulations

A. Mora[1], D. Molnar[1], S. Hocker[1], P. Binkele[1], A. Choudhury[2], R. Mukherjee[2], B. Nestler[2], S. Schmauder[1]

[1] Institute for Materials Testing, Materials Science and Strength of Materials (IMWF), University of Stuttgart, Germany

[2] Institute of Materials and Processes (IMP), University of Applied Sciences, Karlsruhe, Germany

Motivation

Copper, Nickel and Manganese alloyed steels are widely used in power stations as material for pipelines and pressure vessels. These alloys permit higher hardness and tensile stress at high operational temperatures of power stations, which vary between 300 and 450°C. After years of operation hardening can lead to embrittlement and failure.

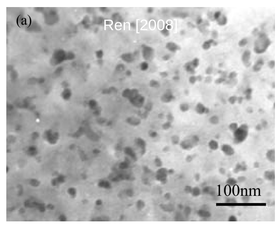

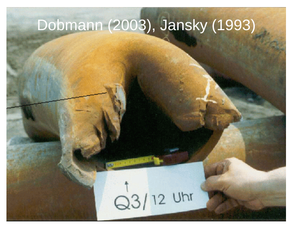

As a result of thermal aging, coherent bcc Cu-rich precipitates nucleate and grow in the α Fe-matrix. After a critical radius of ~ 2 nm, precipitates start a crossover to a fcc crystal structure, where Cu finds its lowest bulk free energy[1].

bcc→	Twinned 9R → 3R →	fcc
$r < 2nm$	$r : 2 - 9nm$	$r > 9nm$

Formation and growth of precipitates in thermally aged Fe-Cu-Ni-Mn alloys at temperatures above 300°C are studied by kinetic Monte Carlo simulations. By means of a thermal activated vacancy diffusion mechanism on a rigid bcc lattice, it is possible to characterize the processes of nucleation, growth, and Ostwald ripening of the Cu-rich clusters for a wide range of temperatures and temporal scales.

Kinetic model

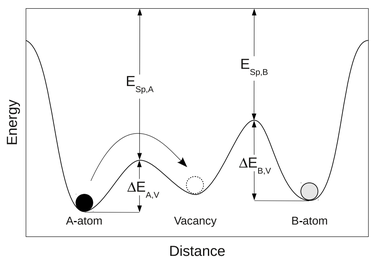

The bcc structure is modeled by a fixed lattice occupied with Fe-,Cu-,Ni-,Mn-atoms and 1 vacancy. The precipitation occurs by atomic diffusion driven by a thermally activated vacancy mechanism[2]

$$\Gamma_{X_j,V} = \nu_{X_j} \exp\left(-\frac{\Delta E_{X_j,V}}{kT}\right),$$

where $X_j \in \{\text{Fe, Cu, Ni, Mn}\}$

$\Gamma_{X_j,V}$: Jump rates for atom X_j and vacancy V

ν_{X_j} : Attempt frequencies

$\Delta E_{X_j,V}$: Activation energies for migration

kT : Boltzmann-constant $\times$ temperature

The activation energies $\Delta E_{X_j,V}$: are strongly dependent on the local arrangement and are calculated separately for each interchange of atomic positions

$$\Delta E_{X_j,V} = E_{Sp,X_j} - \sum_{i=1}^{2}\sum_{k=1}^{4} n^{(i)}_{X_jX_k}\varepsilon^{(i)}_{X_jX_k} - \sum_{i=1}^{2}\sum_{k=1}^{4} n^{(i)}_{VX_k}\varepsilon^{(i)}_{VX_k},$$

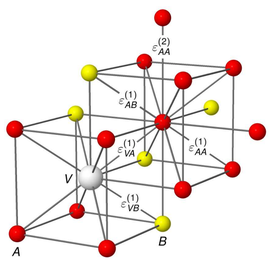

where: $X_j, X_k \in \{\text{Fe, Cu, Ni, Mn}\}$

E_{Sp,X_j} : Saddle point energy

$\varepsilon^{(i)}_{X_jX_k}$: Interatomic energies

$\varepsilon^{(i)}_{VX_k}$: Vacancy interaction energ.

$n^{(i)}_{X_jX_k}$: Occupation numbers

$i = 1$: 8 nearest neighbors

$i = 2$: 6 second nearest neighbors

The energies $E_{Sp,X_j}, \varepsilon^{(i)}_{X_jX_k}, \varepsilon^{(i)}_{VX_k}$: are derived from experimental data, and Ab initio and Calphad calculations[3].

Kinetic-Monte Carlo (KMC) simulations

Fe - Cu 1.5 wt % - Ni 1.3 wt% - Mn 0.95 wt% $\quad T = 500^oC, \quad L = 128, \quad N = 4194304 - 1$ vacancy

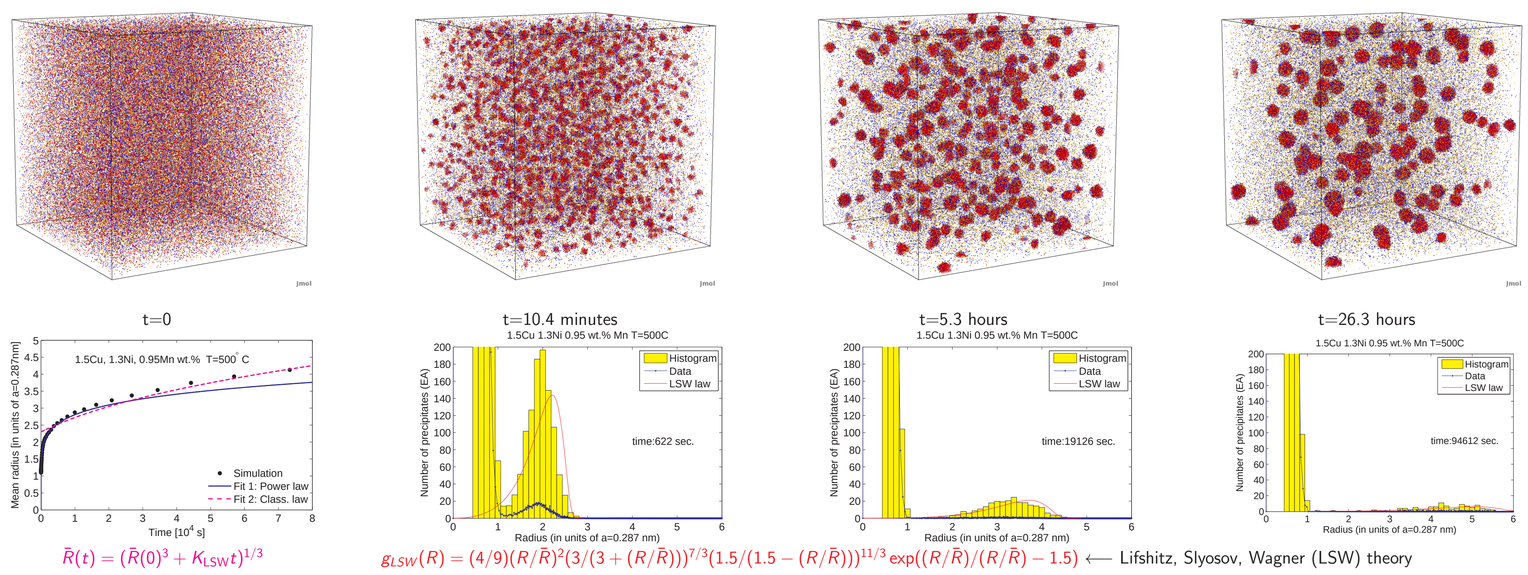

$\bar{R}(t) = (\bar{R}(0)^3 + K_{LSW}t)^{1/3}$

$g_{LSW}(R) = (4/9)(R/\bar{R})^2(3/(3+(R/\bar{R})))^{7/3}(1.5/(1.5-(R/\bar{R})))^{11/3}\exp((R/\bar{R})/(R/\bar{R})-1.5)$ ⟵ Lifshitz, Slyosov, Wagner (LSW) theory

Single precipitate composition

Ni and Mn solute atoms have the tendency to form shells around the precipitates.

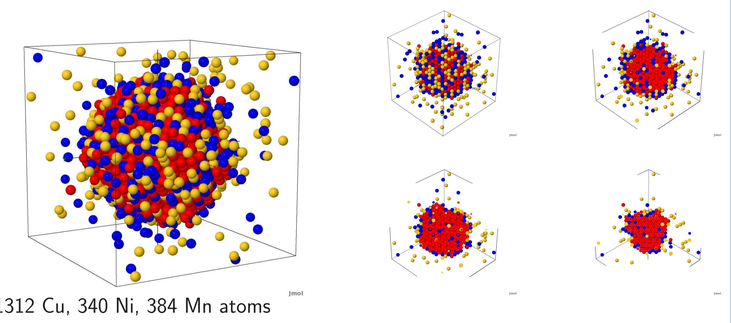

1312 Cu, 340 Ni, 384 Mn atoms

Parametric study

The degree of advancement of the precipitation is measured by $\xi(t) = (C^m_B(t_0) - C^m_B(t)) \,/\, (C^m_B(t_0) - C^m_B(\infty))$ where $C^m_B(t)$ is the solute atom concentration within the solid solution (matrix m) and compared with the Johnson-Mehl-Avrami-Kolmogorov (JMAK) law: $\xi(t) = 1 - \exp\{-(t/\tau)^n\}$ for different temperatures (figure below, left).

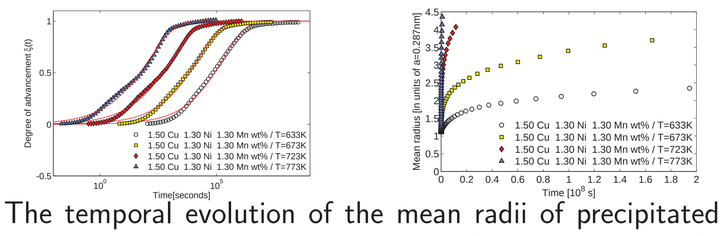

The temporal evolution of the mean radii of precipitated was traced for different temperatures (figure above right).

(1) Fe-Cu: Varying Cu concentration at constant T

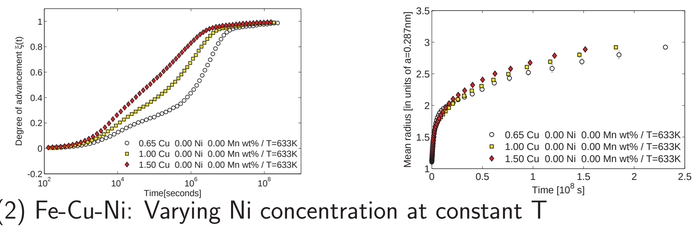

(2) Fe-Cu-Ni: Varying Ni concentration at constant T

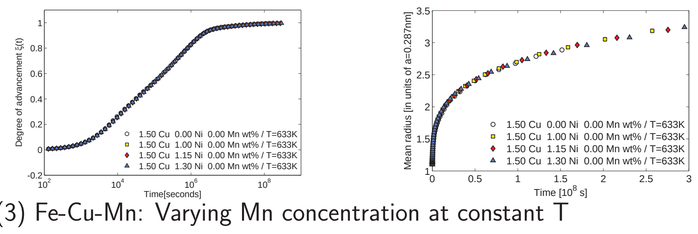

(3) Fe-Cu-Mn: Varying Mn concentration at constant T

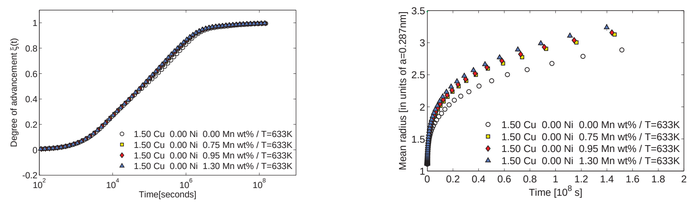

Phase Field Method (PFM) simulations

Phase-field modeling provides the proper framework to complement the atomistic simulations and extend them to larger spatial and temporal scales. We use a quantitative PFM model based on a grand chemical potential formulation[4], which uses the final results of KMC as initial configuration and Calphad data for thermodynamic description of the system. The size and location of each precipitate cluster obtained in the KMC simulations are transfered as input for the phase-field simulations. Interfacial energies are calculated with the broken-bond model and diffusivities are estimated from experimental data reported in literature.

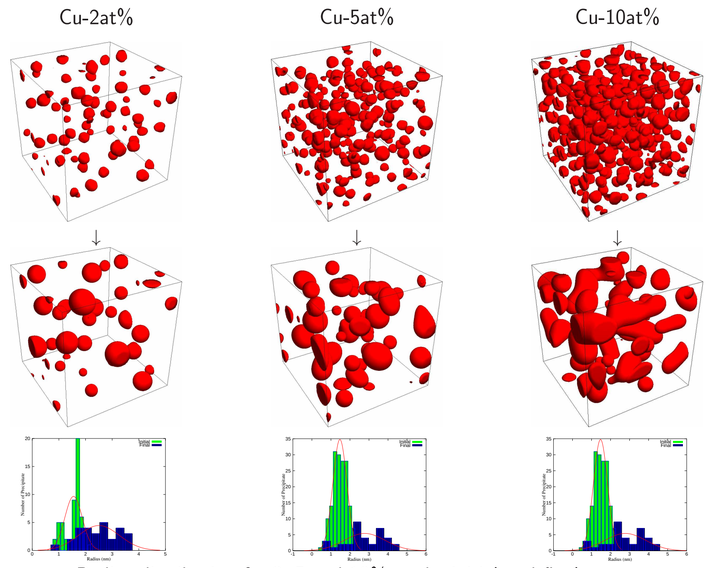

(a) Evolution of the average radius (b) Number of particles versus time

Conclusions

- The atomistic Monte Carlo method allow to simulate coherent precipitation in Fe-Cu-Ni-Mn alloys via a vacancy mechanism. The obtained precipitate radii distributions and the temporal evolution of the mean radii follow approximately the classical LSW theory for Ostwald ripening.
- The parametric study shows that Ni solute atoms do not play a significant role on the precipitation. On the other hand, Mn atoms contribute accelerating the coarsening.
- The phase-field model can be validated quantitatively for the Gibbs-Thomson effect and it also predicts the coarsening kinetics correctly.
- While the Monte Carlo method captures the nucleation of small precipitate clusters, the phase-field model is able to capture the coarsening regime and coalescence events at high volume fraction of precipitates.

Interfacial energies calculations - broken bond model

Interfacial energies between a Cu-rich cluster and the surrounding Fe-rich matrix are calculated using the nearest neighbor broken-bond model[5] which is based on the interatomic energies ε_{AB} :

$$\gamma = n_s z_s \left[\varepsilon_{AB} - \tfrac{1}{2}(\varepsilon_{AA} + \varepsilon_{BB})\right],$$

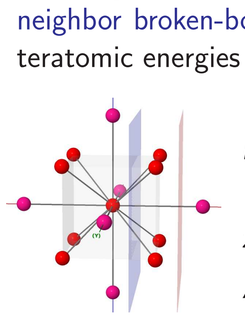

n_s : number of bonds across the interface per atom

z_s : number of surface atoms/unit area

$A, B \in \{\text{Fe, Cu, Ni, Mn}\}$

Interfacial energies for some orientation crystal planes:

$$\gamma_{\{100\}} = \tfrac{1}{a^2}\cdot(4\varepsilon^{(1)}_{AB} + 2\varepsilon^{(2)}_{AB} - 2\varepsilon^{(1)}_{AA} - \varepsilon^{(2)}_{AA} - 2\varepsilon^{(1)}_{BB} - \varepsilon^{(2)}_{BB})$$
$$\gamma_{\{110\}} = \tfrac{\sqrt{2}}{a^2}\cdot(2\varepsilon^{(1)}_{AB} + 2\varepsilon^{(2)}_{AB} - \varepsilon^{(1)}_{AA} - \varepsilon^{(2)}_{AA} - \varepsilon^{(1)}_{BB} - \varepsilon^{(2)}_{BB})$$
$$\gamma_{\{111\}} = \tfrac{\sqrt{3}}{3a^2}\cdot(5\varepsilon^{(1)}_{AB} + 6\varepsilon^{(2)}_{AB} - \tfrac{5}{2}\varepsilon^{(1)}_{AA} - \tfrac{6}{2}\varepsilon^{(2)}_{AA} - \tfrac{5}{2}\varepsilon^{(1)}_{BB} - \tfrac{6}{2}\varepsilon^{(2)}_{BB})$$

γ [J/m^2]	{100}	{110}	{111}
Fe-Cu	0.4834	0.4101	0.4465
Fe-Ni	0.1064	0.0903	0.0983
Fe-Mn	0.1596	0.1355	0.1475
Cu-Ni	0.0443	0.0376	0.0410
Cu-Mn	0.1951	0.2759	0.3379
Ni-Mn	-0.2838	-0.2408	-0.2622

References

[1] Othen, Jenkins, Smith. *Philos.Mag.A*, **70**, 1-24 (1994).

[2] Soisson, Barbu, Martin. *Acta Mater.* **44**, 3789-3800 (1996); Schmauder, Binkele, *Comp. Mater. Sci.*, 24, 42-53 (2002). Soisson, Fu. *Phys.Rev.B* **76**, 214102 (2007)

[3] Molnar, Binkele, Hocker, Schmauder. *Philos.Mag.* **92** 586-607(2012) Mora, Molnar, Hocker, Binkele, Choudhury, Mukherjee, Nestler, Schmauder. *In preparation.*

[4] Choudhury, Nestler, *Phys.Rev.E* **85**, 021602/1-16,(2012).

[5] Janssens, Raabe, Kozeschnik, Miodownik, Nestler *Computational Materials Engineering*. Elsevier (2007).

• *Funding for this project is provided by Deutsche Forschungsgemeinschaft (DFG) under the project number SCHM-746/101-1.*